

ISOTOPIC COMPOSITION OF CARBONATE FACIES IN FORMATIONS OF THE UPPER TRIASSIC CHINLE GROUP, FOUR CORNERS AREA, SOUTHWESTERN UNITED STATES

LAWRENCE H. TANNER¹ AND SPENCER G. LUCAS²

¹ Department of Biological Sciences, Le Moyne College, Syracuse, NY 13203, email: tannerlh@lemoyne.edu;

² New Mexico Museum of Natural History and Science, 1801 Mountain Road, NW, Albuquerque, NM 87104

Abstract—Carbonates of the Ojo Huelos Member of the San Pedro Arroyo Formation include ostracodal limestones, brecciated micritic limestones, vuggy, mottled limestones, peloidal graistones/packstones, pisolitic rudstones and nodular limestones. These lithofacies record deposition in lacustrine, palustrine and alluvial environments. Lacustrine (ostracodal) limestones are isotopically heaviest, with nodular limestones, palustrine limestones and peloidal/psolitic limestones all progressively depleted. We interpret isotopic depletion as a consequence of exposure to atmospheric and soil-derived CO₂ during pedogenic reworking of lacustrine-derived carbonate. Comparison of the Ojo Huelos carbonates to the isotopic composition of similar lithofacies from the Owl Rock Formation (Chinle Group) assists in elucidating the role of pedogenesis in development of the carbonate fabrics in the Ojo Huelos Member. Distinct differences in the isotopic composition of lacustrine and palustrine carbonates from the two formations may or may not reflect differences in climate during deposition.

INTRODUCTION

Lacustrine and palustrine carbonate deposits of the Upper Triassic Chinle Group are of particular interest for the potential wealth of paleoclimate data they contain (Tanner, 2000, 2010; Tanner and Lucas, 2012). Deposition of the formations of the Chinle Group coincided with the northward drift and breakup of Pangea, which had discernible effects on climate and sedimentation in southwestern North America (Dubiel et al., 1991; Parrish, 1993; Olsen, 1997; Clemmensen et al., 1998, Tanner, 2000; Tanner and Lucas, 2007, 2012).

Lacustrine carbonate deposition is commonly, although often incorrectly, associated with a semi-arid climate. While it is true that the aqueous carbonate concentration is likely to be too dilute to facilitate precipitation in more humid climates, overly dry climates are not conducive to maintaining perennial water bodies, and so prevent carbonate sedimentation (Dean, 1981; Cecil, 1990; Platt and Wright, 1991; Sanz et al., 1995; De Wet et al., 1998; Gierlowski-Kordesch, 1998). Semi-arid conditions, however, do indeed favor carbonate precipitation, particularly in closed basins where evaporative concentration results in high levels of alkalinity, a condition that may be met regardless of latitude or altitude. Evidence of semi-aridity is often presented in the lacustrine facies through evaporites or stromatolites interbedded with lacustrine carbonates, recording the climatically driven expansion and contraction of ephemeral water bodies (Platt and Wright, 1991).

Palustrine carbonates, i.e., carbonate muds of low-energy lake margins, ponds in alluvial settings, seasonal wetlands, and some peritidal settings (Platt and Wright, 1991, 1992; Sanz et al., 1995; see Alonso-Zarza, 2003, for a comprehensive review), are also very sensitive to changes in hydrologic regime, and consequently, to variations in precipitation or groundwater levels. Composition and syndimentary features record the moisture availability during the formation and subaerial exposure of the sediments. For example, drier climates will cause more intense desiccation, with consequent brecciated and peloidal fabrics, and formation of microkarst surfaces, while organic-rich facies are more likely to record semi-humid conditions (Platt and Wright, 1992; Alonso-Zarza et al., 1992; Alonso-Zarza, 2003).

The $\delta^{18}\text{O}$ of lacustrine carbonate from hydrologically open lakes may be used for paleotemperature calculations. In closed-basin lakes, $\delta^{18}\text{O}$ and $\delta^{13}\text{C}$ typically exhibit covariance due to enrichment from evaporation and atmospheric exchange. The isotopic composition of palustrine carbonates, however, does not lend itself to paleoclimatic interpretation,

as the potential controlling factors are many, and include the isotopic composition of the original lake waters, the composition of potentially interacting shallow groundwaters, the presence and activity of vegetation on the sediment surface, and the extent and depth of pedogenic modification (Alonso-Zarza, 2003; Tanner, 2010).

This paper presents new isotopic data from interbedded lacustrine-palustrine and alluvial limestones of the Upper Triassic (Carnian) Ojo Huelos Member of the San Pedro Arroyo Formation (Chinle Group) in central New Mexico, USA. Thin section blanks of carbonate facies from the Ojo Huelos Member were sampled and analyzed for $\delta^{13}\text{C}$ and $\delta^{18}\text{O}$ by Coastal Science Laboratories, Houston, Texas. Results are reported (in ppt relative to VPDB). As some of the carbonate facies in the Ojo Huelos Member bear striking similarity to those of the younger (Norian) Owl Rock Formation (Chinle Group), we compare these two formations and discuss them in the context of Late Triassic climatic change in the Colorado Plateau region of the American Southwest.

OJO HUELOS CARBONATES

Setting and Stratigraphy

The importance of the paleoclimatic interpretation of the Ojo Huelos Member of the San Pedro Arroyo Formation, a distinctive carbonate-rich unit that crops out in central New Mexico (Fig. 1), derives from its stratigraphic position relative to other Chinle Group formations for which paleoclimate information is available (Fig. 2). In the western United States, the Adamanian (late Carnian) Ojo Huelos Member is the oldest distinctively carbonate-rich unit that occurs in the Chinle Group (Lucas, 1991). The member consists mainly of micritic lime mudstones, ostracodal wackestones to grainstones, peloidal grainstones and distinctive pisolitic rudstones, interbedded with fine-grained siliciclastic mudstones. The San Pedro Arroyo Formation is underlain by alluvial strata of the Shinarump Formation, which display features suggesting deposition during subhumid conditions (Dubiel et al. 1991; Parrish 1993; Dubiel 1994; Tanner and Lucas, 2007). Although Upper Triassic strata overlying the San Pedro Arroyo Formation are not preserved in central New Mexico, Norian-age strata that occupy that stratigraphic position elsewhere, e.g., the Petrified Forest Formation (Blue Mesa Member), lack distinct carbonate-rich depositional facies. Consequently, the San Pedro Arroyo Formation occupies an important position with regard to the evolution of the paleogeography and paleoclimate of the American Southwest during the Late Triassic.

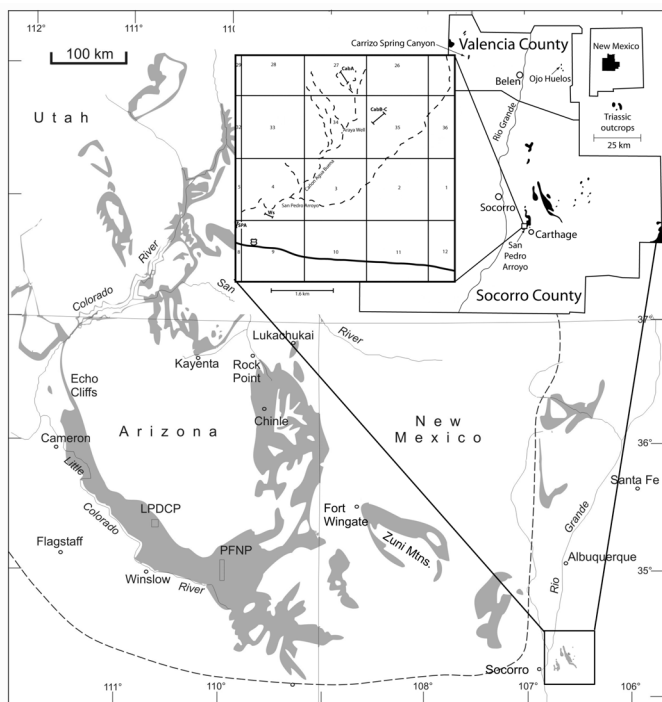


FIGURE 1. Location map of outcrops of the Chinle Group formations (shaded) in the Four Corners area with inset map showing location of Ojo Huelos Member outcrops in New Mexico (Spielmann and Lucas, 2009). PFNP = Petrified Forest National Park.

Ojo Huelos lithofacies

Ostracodal limestones

The invertebrate fauna of the Ojo Huelos carbonates consists almosts entirely of darwinuloid (freshwater) ostracodes (Heckert and Lucas, 2002). Where common, their shells are hosted mainly by well-bioturbated micritic wackestones and packstones (Fig. 3A). Coarser-grained beds (grainstones and packstones) contain other bioclasts, such as fish bones and scales, and tend to be enriched in organic matter. Tanner and Lucas (2012) interpreted the ostracodal limestones as lacustrine deposits with coarsening upward beds as shoaling-upward shoreline sequences.

The isotopic composition of two samples of ostracodal limestone are consistent at $\delta^{13}\text{C} = -3.5, -4.7 \text{‰}$ and $\delta^{18}\text{O} = -5.9, -6.1 \text{‰}$. These values demonstrate little evaporative isotopic enrichment and therefore are consistent with the typical signatures of carbonate precipitated in a hydrologically open lacustrine basin (Talbot, 1990; Talbot and Kelts, 1990; Platt, 1992; Tanner, 2010).

Micritic brecciated limestones

In the Ojo Huelos Member, dense, mottled micritic limestone occurs in beds ranging from 0.2 m to 1.1 m in thickness (Fig. 3B). The beds are tabular to lenticular, and typically interbedded with mudstone. The most common characteristic among beds of this lithology is a brecciated fabric throughout all or part of the bed, comprising angular domains of micrite up to 10 cm in diameter, although the domain boundaries vary from sharp to diffuse, separated by mm-wide to cm-wide veins of equant crystals of microspar to sparry calcite. In some places, the domains consist of fine, dense micrite that is intensely brecciated on a sub-mm scale to form 0.2 mm to 2 mm clasts separated by sparry veins. In other places, the domains may display an undifferentiated massive to (less-common) clotted-peloidal fabric with circumgranular cracking, comprising micrite that is silty to slightly argillaceous. Subvertical root traces,

downward tapering and branching, are common from the tops of beds. Tanner and Lucas (2012) interpreted the micritic limestone facies as carbonate sediments deposited in shallow lacustrine to wetland settings and reworked to varying extents by pedogenic processes.

The isotopic composition of six samples of faintly to pervasively brecciated micritic limestone are relatively uniform; $\delta^{13}\text{C}$ ranges from -7.5 to -5.6‰ (mean = -6.3‰), $\delta^{18}\text{O}$ ranges from -7.7 to -6.1‰ (mean = -6.5‰) and is significantly depleted relative to the lacustrine limestone facies described above. Numerous authors have noted that in laterally adjacent environments, lacustrine carbonate tends to be isotopically heavier than the carbonate of laterally equivalent palustrine facies, due to the mixing of original isotopically heavy lacustrine carbonate with lighter carbonate precipitated in equilibrium with atmospheric CO_2 and/or meteoric groundwaters (Platt, 1989; Tanner, 2000; Alonso-Zarza, 2003).

Vuggy limestone

Tanner and Lucas (2012) noted the occurrence of distinctive beds of brownish-yellow, mottled limestone at the base of the type section of the Ojo Huelos Member at Ojo Huelos (Fig. 3C). This facies is distinguished by vertically elongated cavities and gray-brown, branching mottles. The matrix of the facies consists of dark micritic calcite with irregular hematite stains and irregularly disseminated fine organic matter, and locally contains abundant ostracodes. The fabric of the micrite is generally quite uniform, comprising crystallites $1 \mu\text{m}$ to $2 \mu\text{m}$ across. Millimeter-scale, horizontal veins of calcite spar cross-cut the micrite matrix. The upper surface of the bed is fine micrite that is less dense than the underlying matrix, and lacks ostracodes or sparry veins.

The oxygen isotope composition of the calcite in the porous limestone facies at Ojo Huelos is significantly depleted ($\delta^{13}\text{C} = -4.7 \text{‰}$, $\delta^{18}\text{O} = -16.2 \text{‰}$), which is anomalous for the Ojo Huelos carbonates and suggests precipitation from groundwater rather than meteoric water. This is consistent with the microfabric of equant, uniform-size crystallites, which lacks evidence of cyanobacterial influence, such as tubiform crusts or filaments (cf. Jannsen et al., 1999; Merz-Preiß and Riding, 1999). Consequently, Tanner and Lucas (2012) interpreted this facies as carbonate precipitated from spring flow as a tufa (sensu Ford and Pedley, 1996).

Peloidal grainstone/packstone

This facies is similar to the granular limestone facies of Alonso-Zarza et al. (2011). It consists of a framework of well-rounded to subangular micrite grains in a matrix that varies from mostly detrital, silt to sand-size grains of siliciclastic particles to a combination of sand-size grains of quartz, smaller micritic calcite clasts and bioclasts (fragments of ostracods, and phosphatic fish scales and bones) cemented by sparry calcite (Fig. 3D). Larger pisoids (up to 8 mm) comprise a minor proportion of the grain framework. The framework grains in the grainstones of this facies, which are cemented by calcite, typically display point contacts, whereas the peloidal packstones, which have a clayey matrix, show complex grain contacts, ranging from concavo-convex to sutured. Tanner and Lucas (2012) noted the presence of the mixed carbonate/siliciclastic grain irregularly-shaped, hematite-stained argillaceous clasts, and suggested that this facies records erosion and redeposition of palustrine carbonate by traction currents.

The isotopic composition of two samples of peloidal limestone matches well the composition of the micritic to brecciated limestone facies described above ($\delta^{13}\text{C} = -7.5, -7.1 \text{‰}$; $\delta^{18}\text{O} = -6.3, -6.0 \text{‰}$), suggesting that the peloidal limestone clasts were derived from intense brecciation of palustrine carbonate.

Pisolite

Somewhat similar to the peloidal facies are the pisolitic limestones (Fig. 3E). These are meter-scale beds of rudstone, massive to crudely stratified, with a framework that consists of pisoids. Individual

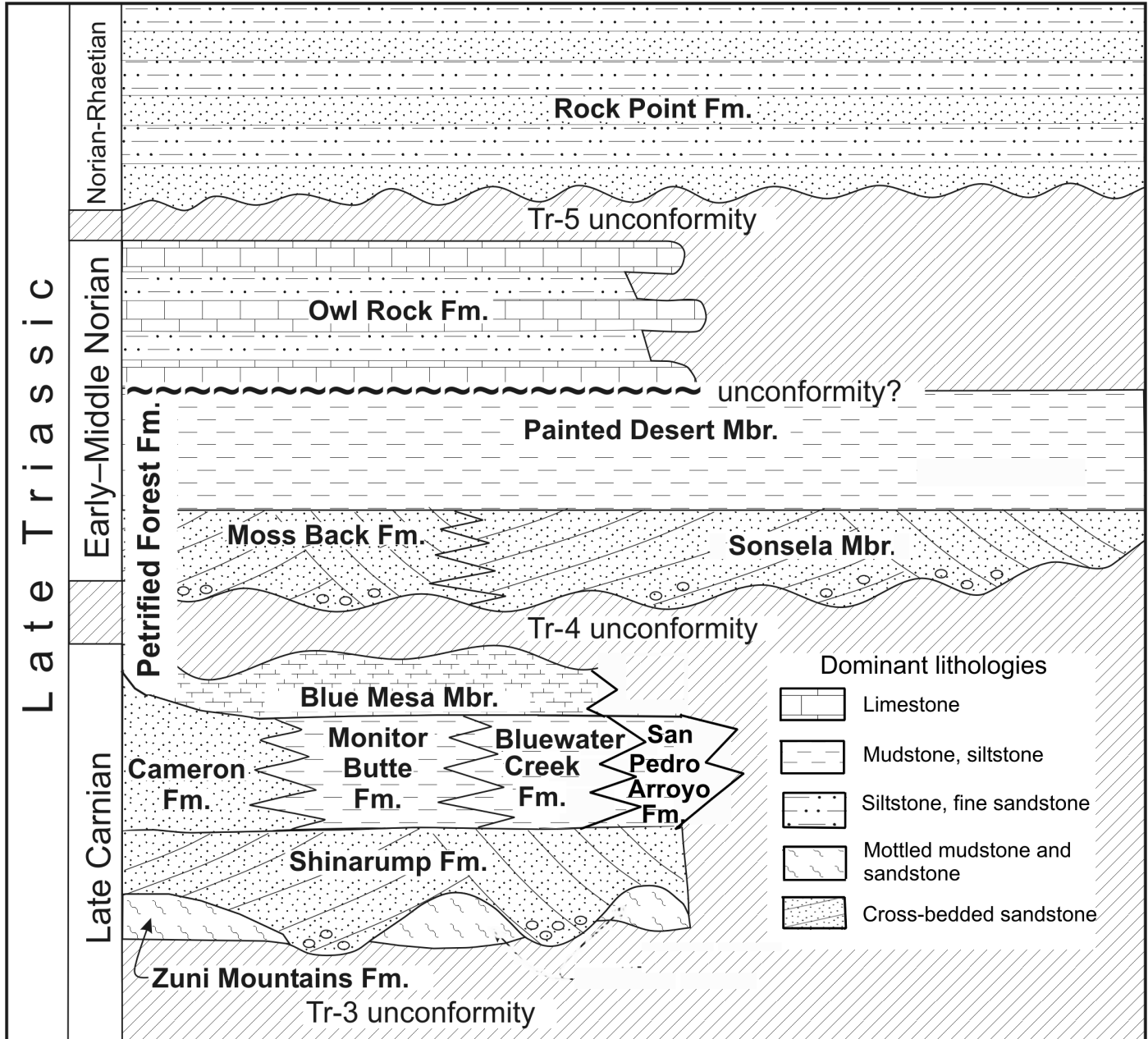


FIGURE 2. Stratigraphy of the Chinle Group across the Four Corners area.

pisoids are up to 3 cm in diameter and display concentric layering and hematite staining. The pisoids are set in a matrix that consists of a mix of sand-size grains of quartz with some chert and smaller calcareous mudstone clasts, all in a sparry calcite matrix. Tanner and Lucas (2012) interpreted the pisoids as originating through intense pedogenic reworking of palustrine carbonate; the pisoids were subsequently eroded and redeposited by fluvial processes, as described above for the peloidal grainstone/packstone facies, as the gravel bars of energetic, high-bedload streams.

The isotopic composition of two samples of calcite from pisolites varied widely ($\delta^{13}\text{C} = -8.4, -6.3 \text{‰}$; $\delta^{18}\text{O} = -9.0, -5.7 \text{‰}$), but overlap with both the micritic/brecciated limestone and peloidal limestone facies, suggesting a common source of carbonate; i.e., the palustrine carbonate was the source material for the peloids and pisoids in the facies described above.

Nodular limestones

Nodular limestones, interpreted by Tanner and Lucas (2012) as calcretes, occur in the Ojo Huelos Member interbedded with or overlying lacustrine and palustrine limestones (Fig. 3F; Tanner and Lucas, 2012). The calcretes are hosted by mudstones and typically occur near the top of the Ojo Huelos Member. These nodular limestones typically display extensive root traces and weather to form prominent benches on slopes. The mudstone-hosted calcareous nodule horizons are less than 1 meter thick. The micritic nodules vary in shape from subspherical to irregularly globular (botryoidal), are several cm in diameter, and typically have diffuse boundaries.

The isotopic composition of two samples of calcite from the nodular limestone varies widely ($\delta^{13}\text{C} = -5.3, -3.6 \text{‰}$; $\delta^{18}\text{O} = -9.1, -5.4 \text{‰}$), but overlaps with other limestone facies in this formation described above, in particular, the ostracodal limestones. Consequently, we sug-

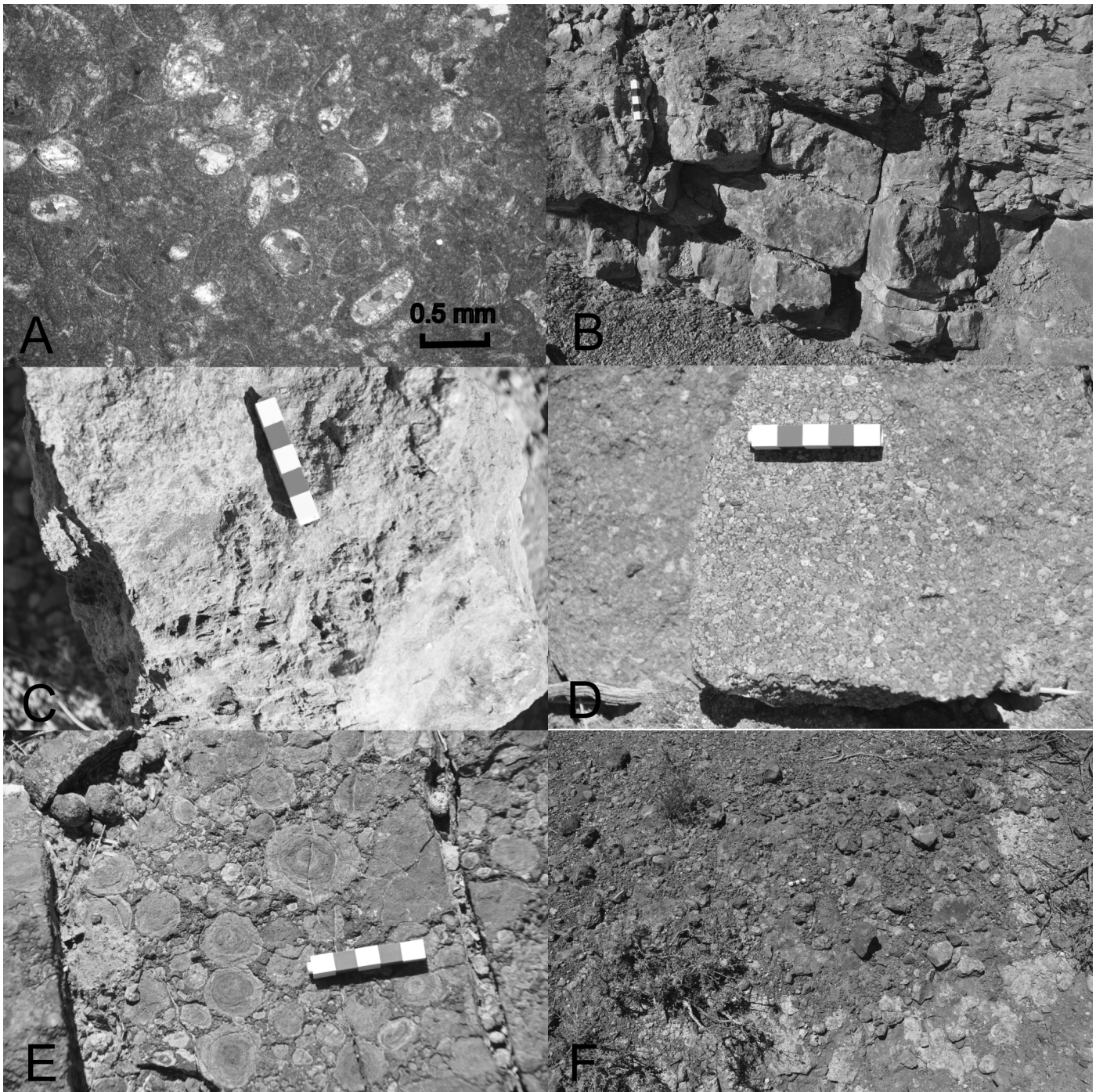


FIGURE 3. Carbonate lithofacies of the Ojo Huelos Member (San Pedro Arroyo Formation). Scale bar in **B-F** is 5 cm. **A**, Ostracodal packstone from the type section of the Ojo Huelos Member. **B**, Mottled, brecciated micritic limestone, the most common lithofacies of the Ojo Huelos Member. **C**, Vuggy limestone from the base of the type section. **D**, Peloidal packstone consists mainly of clasts of micrite with subordinate mudstone. **E**, Pisolitic rudstone is a prominent facies only locally in the Ojo Huelos Member. The pisolite consists of concentric layered pisoids in sandy, calcite matrix. **F**, Nodular limestone horizon hosted by mottled mudstone typically occurs in the upper part of the Ojo Huelos Member.

gest that the carbonate in the nodular limestones represents, at least in part, lacustrine carbonate sediment, rather than solely recording carbonate accumulation in the B horizon of a soil profile.

OWL ROCK FORMATION

Setting and Stratigraphy

The Owl Rock Formation comprises up to 150 m of interbedded pink to red mudstones, siltstones, fine-grained sandstones, and lime-

stones of late Revueltian (approximately middle Norian) age. These strata crop out in northern Arizona, northwestern New Mexico, and southern Utah (Stewart et al., 1972; Lucas and Huber, 1994; Lucas et al., 1997). Dubiel et al. (1991) noted that the contact between the Owl Rock Formation and the underlying Painted Desert Member of the PFF appears disconformable, being marked in many places by the presence of a thick intrabasinal conglomerate comprising mainly reworked calcrete clasts and unionid bivalves.

The upper part of the formation is characterized by ledge-forming

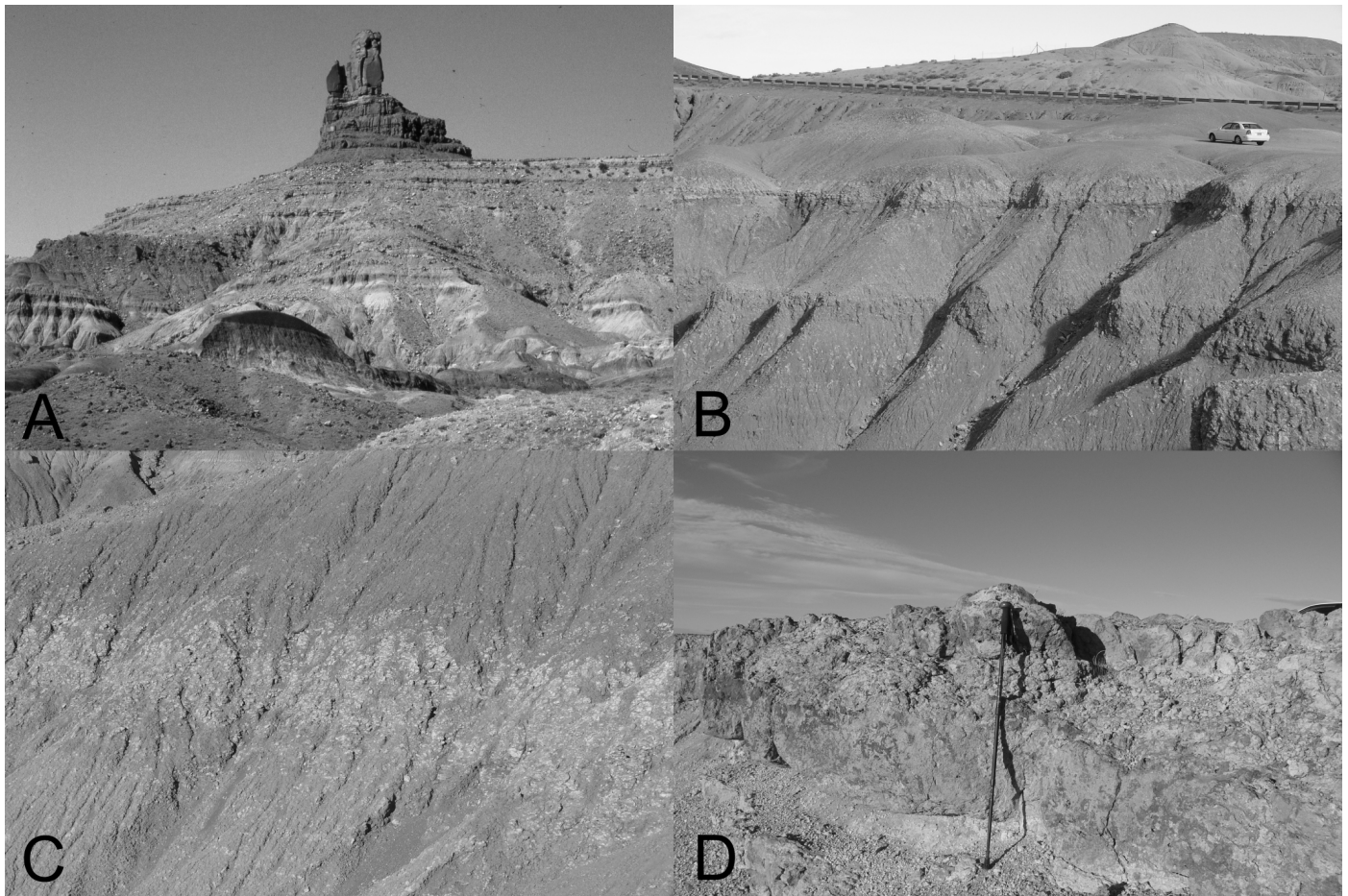


FIGURE 4. Features of the Owl Rock Formation. **A**, Type section of the Owl Rock Formation near Kayenta, Arizona. The formation consists of interbedded limestone ledges and mudstones. The darker mudstones of the Rock Point Formation overlie the Owl Rock Formation abruptly at the top of the cliff. **B**, Cliff section of the Owl Rock Formation at the southern end of the Echo Cliffs, north of Cameron, Arizona. Immature calcrete horizons occur in the lower part of the section; calcrete maturity increases upward. **C**, Detail of immature calcrete from lower part of Owl Rock Formation. **D**, Limestone ledges in the uppermost Owl Rock Formation typically exhibit brecciated fabric, mottling and chertification.

beds of limestone, typically less than one meter thick. Earlier workers (Blakey and Gubitosa, 1983; Dubiel, 1989, 1993) described these as lacustrine limestones and interpreted them as deposits of a large lacustrine system centered on the Four Corners region. Other workers, however, recognized pervasive pedogenic fabrics in these beds and suggested that they represent mature (stage III and IV) calcretes and palustrine carbonates (Lucas and Anderson, 1993, Lucas et al., 1997; Tanner, 2000; Tanner and Lucas, 2007). The formation is truncated by a diachronous unconformity (the Tr-5 unconformity) that is overlain in the eastern portion of the outcrop belt by the Rock Point Formation, of early-middle Apachean (Norian to possibly early Rhaetian) age (Lucas et al., 1997), and to the west by the Dinosaur Canyon Member of the Moenave Formation of late Apachean-Wassonian (Rhaetian-Hettangian) age (Lucas and Tanner, 2007; Tanner and Lucas, 2007).

Previous Work

The sedimentology of the Owl Rock Formation was studied in detail by Tanner (2000), who found that at the type section near Kayenta, Arizona, there are distinct differences in the types of paleosols between the lower and upper strata of the formation. In the lower part of the formation, thick mudstone beds lack discernible horizonation and host m-scale immature (stage II to III) calcrete horizons. In contrast, the upper part of the Owl Rock Formation is characterized by ledges of limestone that display pronounced lateral variation in character. Features

such as oscillation ripple lamination, desiccation polygons, and burrowing are laterally gradational with limestones that display brecciated to peloidal fabrics, spar-filled circumgranular cracks, and root channels. Tanner (2000) interpreted the range of features as the record of variation between subaqueous (lacustrine) to subaerial (palustrine/alluvial) deposition across an alluvial plain; and the brecciated beds as palustrine limestones, formed by deposition of carbonates in ponds on a sediment-starved floodplain that was subjected to intense pedogenesis during base-level fluctuations (Platt, 1992; Platt and Wright, 1992; Armenteros et al., 1997; Alonso-Zarza, 2003).

Tanner and Lucas (2006) described additional pedogenic features of the Owl Rock Formation at other localities (e.g., in the Echo Cliffs, at Little Painted Desert County Park, and near Lukachukai, Arizona). At the southern end of the Echo Cliffs, for example, the contact with the Petrified Forest Formation is marked by thick-bedded intrabasinal conglomerate consisting largely of reworked calcrete with mudstone clasts and chert pebbles. The lower part of the Owl Rock Formation contains thick (up to 5 m) calcretes that are stage II to III and exhibit obvious lateral gradations between stages over distances of hundreds of meters. The upper Owl Rock Formation is characterized by ledge-forming calcareous beds that, like the Ojo Huelos carbonates, typically have abrupt contacts and scoured bases with tens of cm of relief. Also, like the Ojo Huelos carbonates, these ledge-forming beds are generally mottled, contain pisoids and commonly form multi-storeyed bodies

Owl Rock Isotopes

Lapped slabs of lacustrine-palustrine carbonate facies and pedogenic nodules from the Owl Rock Formation were sampled and analyzed for $\delta^{13}\text{C}$ and $\delta^{18}\text{O}$ by Coastal Science Laboratories, Houston, Texas. Results were reported (in ppt relative to PDB) by Tanner (2000). Micrite from two samples of the laminated lacustrine limestone facies at the Owl Rock type locality contains carbonate with mean $\delta^{13}\text{C} = -2.8 \text{‰}$, and mean $\delta^{18}\text{O} = -0.6 \text{‰}$. The brecciated palustrine facies from the Owl Rock section is represented by 16 samples, mostly from the micritic clasts, with mean $\delta^{13}\text{C} = -4.5 \text{‰}$, and mean $\delta^{18}\text{O} = -2.7 \text{‰}$. Massive micrite from five samples of pedogenic nodules from the Echo Cliffs and Owl Rock contains carbonate with a mean $\delta^{13}\text{C} = -7.4 \text{‰}$, and a mean $\delta^{18}\text{O} = -5.7 \text{‰}$.

COMPARISON AND INTERPRETATION

As discussed by Tanner (2000), the composition of the laminated limestone facies represents the signature of lacustrine carbonate precipitated from evolved evaporation-enriched lacustrine waters (Talbot 1990; Platt 1992), an interpretation that is consistent with the presence of (rare) calcite pseudomorphs of gypsum in the Owl Rock carbonates. In contrast, the samples of pedogenic micrite appear to represent carbonate precipitated in a soil profile at equilibrium conditions with atmospheric CO_2 (Mora et al., 1993; Tanner, 2000). These values are consistent with other values reported from Late Triassic pedogenic calcretes (Suchecky et al., 1988; Cerling, 1991; Tanner, 1996). The composition of the brecciated facies is generally intermediate between that of unaltered lacustrine carbonate and of pedogenic carbonate, suggesting mixing of original isotopically heavy lacustrine carbonate with lighter carbonate precipitated in equilibrium with atmospheric CO_2 and/or meteoric groundwaters. The wide range of isotopic values for the brecciated facies reflects variations in carbonate available during multiple stages of carbonate precipitation, including the original (heavy) lacustrine carbonate, lighter pedogenic carbonate, and additional possible contributions from meteoric phreatic waters at a range of temperatures. As noted by Tanner (2000), other studies of the isotopic composition of palustrine carbonate have yielded similarly variable carbon-isotope values (Platt, 1989, 1992).

For the most part, the isotopic composition of the Ojo Huelos carbonate facies is distinctly different, being generally depleted with respect to ^{13}C in particular, relative to analogous facies in the Owl Rock Formation. For example, the ostracodal limestones in the Ojo Huelos Member, which are unambiguously lacustrine, average $\delta^{13}\text{C} = -4.1 \text{‰}$, and mean $\delta^{18}\text{O} = -6.1 \text{‰}$, compared to $\delta^{13}\text{C} = -2.8 \text{‰}$, and mean $\delta^{18}\text{O} = -0.6 \text{‰}$ for the Owl Rock lacustrine limestones. As discussed above, Tanner (2000) interpreted the Owl Rock carbonates as precipitated in lake waters that were considerably enriched by evaporation, whereas there is no evidence of this (e.g., evaporates or evaporate pseudomorphs) in the Ojo Huelos Member. The isotopic difference between the two formations could signify a drier climate during Owl Rock deposition in the Norian, but equally well could simply record hydrologic differences between the depositional settings (Tanner, 2010).

The difference in enrichment of the primary lacustrine carbonate also explains the disparity in the composition of the brecciated palustrine carbonate; Ojo Huelos palustrine carbonates have mean $\delta^{13}\text{C} = -6.3 \text{‰}$, and mean $\delta^{18}\text{O} = -6.5 \text{‰}$, compared to the much more enriched Owl Rock values of $\delta^{13}\text{C} = -4.5 \text{‰}$, and $\delta^{18}\text{O} = -2.7 \text{‰}$. As the isotopic signature in the palustrine carbonate is partially inherited from the original lacustrine sediment, subsequently modified by pedogenesis, the evaporatively enriched lake waters during Owl Rock deposition were translated to the more enriched palustrine carbonate in the Owl Rock rather than in the Ojo Huelos.

TABLE 1. Isotopic analyses sorted by lithofacies. Sample localities as follows: **OH**, Ojo Huelos; **CAB**, Cañon Agua Buena; **SPA**, San Pedro Arroyo; **W**, Weber; **CAR**, Carrizo Spring. Numbers refer to position in measured section. Values reported relative to VPDB standard, $\pm 0.2 \text{‰}$.

Sample	Locality	lithofacies	environment	$\delta^{13}\text{C}$	$\delta^{18}\text{O}$
OH3	Ojo Huelos	porous limestone	hot spring	-4.7	-16.2
CAB-6	Cañon Agua Buena	pisolite	fluvial	-6.3	-9
SPA15	San Pedro Arroyo	pisolite	fluvial	-8.4	-5.7
CAB-16	Cañon Agua Buena	peloidal grainstone	fluvial	-7.5	-6.3
CAB-17	Cañon Agua Buena	peloidal limestone	fluvial	-7.1	-6
OH-14	Ojo Huelos	nodular limestone	calcrete (?)	-3.6	-5.4
CAB-23	Cañon Agua Buena	nodular limestone	calcrete	-5.3	-9.1
SPA-6	San Pedro Arroyo	micritic limestone	palustrine	-6.9	-6.1
SPA-9	San Pedro Arroyo	micritic limestone	palustrine	-7	-5.4
SPA-1	San Pedro Arroyo	micritic limestone	palustrine	-7.1	-6
OH-5	Ojo Huelos	micritic limestone	palustrine	-5.2	-6.3
CAR-13	Carrizo Spring	micritic limestone	palustrine	-7.5	-6.1
CAR-12	Carrizo Spring	micritic limestone	palustrine	-6.2	-6.9
OH-9	Ojo Huelos	ostracodal limestone	lacustrine	-3.5	-5.9
OH-12	Ojo Huelos	ostracodal limestone	lacustrine	-4.7	-6.1

The greatest disparity in isotopic composition between the two formations exists in the comparison of the calcretes. Owl Rock calcretes display typical pedogenic carbonate features, such as gradational contacts and vertically stacked nodules; pedogenic carbonate from the Owl Rock Formation averages $\delta^{13}\text{C} = -7.4 \text{‰}$, typical of Upper Triassic pedogenic calcretes, as described above. The nodular limestone facies of the Ojo Huelos Member, in contrast, is isotopically heavier, at mean $\delta^{13}\text{C} = -4.9 \text{‰}$, and lacks the typical features of a calcrete profile seen in the Owl Rock Formation. Rather, the Ojo Huelos nodular limestones are more similar in isotopic composition to the Ojo Huelos lacustrine limestones. Consequently, we conclude that the nodular limestones were deposited initially as lacustrine carbonate, although subsequently modified by pedogenesis, rather than accumulating in the Bk horizon of an aridisol. Indeed, the Ojo Huelos lithofacies most similar compositionally to the Owl Rock calcretes are the peloidal and pisolite facies, at mean $\delta^{13}\text{C} = -7.3$ and -7.4‰ , and mean $\delta^{18}\text{O} = -6.1$ and -7.3‰ , respectively. These data, and the comparison to the Owl Rock calcretes, support the conclusion of Tanner and Lucas (2012) that the individual clasts in the peloidal and pisolitic facies originated in a soil environment through heavy pedogenic modification of lacustrine/palustrine carbonate.

CONCLUSIONS

The isotopic composition of the Ojo Huelos carbonates vary considerably by lithofacies, although there is significant overlap among the various carbonate types. The heaviest carbonate is found in the ostracodal limestones, deposited in a lacustrine environment. This lacustrine carbonate was the source carbonate for the other Ojo Huelos lithofacies, but the carbonate was progressively depleted by pedogenic exposure to atmospheric and soil CO_2 in the nodular, palustrine, peloidal and psilotic limestones, respectively. Comparison to the Owl Rock carbonates is instructive in that the pronounced separation of lacustrine, palustrine and pedogenic carbonate in this formation helps to clarify the role of pedogenic alteration in determining the ultimate isotopic composition of specific lithofacies.

ACKNOWLEDGMENTS

The New Mexico Museum of Natural History and Science Foundation provided generous funding for the isotopic analyses described herein. Assistance in the field from Andrew Heckert and Justin Spielmann is gratefully acknowledged. Helpful comments were provided during the review process by Ana Alonso-Zarza and Andrew Heckert.

REFERENCES

- Alonso-Zarza, A.M., 2003, Palaeoenvironmental significance of palustrine carbonates and calcretes in the geological record: *Earth-Science Reviews*, v. 60, p. 261-298.
- Alonso-Zarza, A.M., Calvo, J.P., and García del Cura, M.A., 1992, Palustrine sedimentation and associated features --- grainification and pseudomicrokarst --- in the Middle Miocene (Intermediate Unit) of the Madrid Basin, Spain: *Sedimentary Geology*, v. 76, p. 43-61.
- Alonso-Zarza, A.M., Genise, J.F., and Verde, M., 2011, Sedimentology, diagenesis and ichnology of Cretaceous and Palaeogene calcretes and palustrine carbonates from Uruguay: *Sedimentary Geology*, v. 236, p. 45-61.
- Armenteros, I., Daley, B., and Garcia, E., 1997, Lacustrine and palustrine facies in the Bembridge Limestone (late Eocene, Hampshire Basin) of the Isle of Wight, southern England: *Palaeogeography, Palaeoclimatology, Palaeoecology*, v. 128, p. 111-132.
- Blakey, R.C. and Gubitosa, R., 1983, Late Triassic paleogeography and depositional history of the Chinle Formation, southern Utah and northern Arizona; *in* Reynolds, M.W., and Dolly, E.D., eds., Mesozoic paleogeography of the west-central United States: Denver, Rocky Mountain Section SEPM, p. 57-76.
- Cecil, C.B., 1990, Paleoclimate controls on stratigraphic repetition of chemical and siliciclastic rocks: *Geology*, v. 18, p. 533-536.
- Cerling, T.E., 1991, Carbon dioxide in the atmosphere: evidence from Cenozoic and Mesozoic paleosols: *American Journal of Science*, v. 291, p. 377-400.
- Clemmensen, L.B., Kent, D.V., and Jenkins, F.A., Jr., 1998, A Late Triassic lake system in East Greenland: facies, depositional cycles and palaeoclimate: *Palaeogeography, Palaeoclimatology, Palaeoecology*, v. 140, p. 135-159.
- Dean, W.E., 1981, Carbonate minerals and organic matter in sediments of modern north temperate hard-water lakes: *Society of Economic Paleontologists and Mineralogists, Special Publication 31*, p. 213-231.
- De Wet, C., Yocum, D.A., and Mora, C., 1998, Carbonate lakes in closed basins: sensitive indicators of climate and tectonics: an example from the Gettysburg Basin (Triassic), Pennsylvania, USA; *in* Stanley, K.W., and McCabe, P.J., eds., Role of eustasy, climate and tectonism in continental rocks: *Society of Economic Paleontologists and Mineralogists, Special Publication 59*, p. 191-209.
- Dubiel, R.F., 1989, Depositional and paleoclimatic setting of the Upper Triassic Chinle Formation, Colorado Plateau; *in* Lucas, S.G., and Hunt, A.P., eds., Dawn of the age of dinosaurs in the American Southwest: Albuquerque, New Mexico Museum of Natural History, p. 171-187.
- Dubiel, R.F., 1993, Depositional setting of the Owl Rock Member of the Upper Triassic Chinle Formation, Petrified Forest National Park and vicinity, Arizona; *New Mexico Museum of Natural History and Science, Bulletin 3*, p. 117-121.
- Dubiel, R.F., 1994, Triassic deposystems, paleogeography, and paleoclimate of the Western Interior; *in* Caputo, M.V., Peterson, J.A., and Franczyk, K.J., eds., Mesozoic systems of the Rocky Mountain region, USA: Denver, Colorado, Rocky Mountain Section SEPM, p. 133-168.
- Dubiel, R.F., Parrish, J.T., Parrish, J.M., and Good, S.C., 1991, The Pangaeon megamonsoon --- evidence from the Upper Triassic Chinle Formation, Colorado Plateau: *Palaios*, v. 6, p. 347-370.
- Ford, T.D., and Pedley, H.M., 1996, A review of tufa and travertine deposits of the world: *Earth-Science Reviews*, v. 41, p. 117-175.
- Gierlowski-Kordesch, E.H., 1998, Carbonate deposition in an ephemeral siliciclastic alluvial system: Jurassic Shuttle Meadow Formation, Newark Supergroup, Hartford Basin, USA: *Palaeogeography, Palaeoclimatology, Palaeoecology*, v. 140, p. 161-184.
- Heckert, A.B., and Lucas, S.G., 2002, The microfauna of the Upper Triassic Ojo Huelos Member, San Pedro Arroyo Formation, central New Mexico: *New Mexico Museum of Natural History and Science, Bulletin 21*, p. 77-85.
- Janssen, A., Swennen, R., Podoor, N., and Keppens, E., 1999, Biological and diagenetic influence in Recent and fossil tufa deposits from Belgium: *Sedimentary Geology*, v. 126, p. 75-95.
- Lucas, S.G., 1991, Triassic stratigraphy, paleontology and correlation, south-central New Mexico: *New Mexico Geological Society, Guidebook 42*, p. 243-259.
- Lucas, S.G., and Anderson, O.J., 1993, Calcretes of the Upper Triassic Owl Rock Formation, Colorado Plateau: *New Mexico Museum of Natural History and Science, Bulletin 3*, p. G32-G41.
- Lucas, S.G., and Huber, P., 1994, Sequence stratigraphic correlation of Upper Triassic marine and nonmarine strata, western United States and Europe; *in* Embry, A.F., Beauchamp, B., and Glass, D.J., eds., Pangea: Global Environments and Resources: Canadian Association Petroleum Geologists, *Memoir 17*, p. 241-254.
- Lucas, S. G. and Tanner, L. H., 2007, Tetrapod biostratigraphy and biochronology of the Triassic-Jurassic transition on the southern Colorado Plateau, USA: *Palaeogeography, Palaeoclimatology, Palaeoecology*, v. 244, p. 242-256.
- Lucas, S.G., Heckert, A.B., Estep, J.W., and Anderson, O.J., 1997, Stratigraphy of the Upper Triassic Chinle Group, Four Corners region: *New Mexico Geological Society, Guidebook 48*, p. 81-108.
- Merz-Preiß, M., and Riding, R., 1999, Cyanobacterial tufa calcification in two freshwater streams: Ambient environment, chemical thresholds and biological processes: *Sedimentary Geology*, v. 126, p. 103-124.
- Mora, C.I., Fastovsky, D.E., and Driese, S.G., 1993, Geochemistry and stable isotopes of paleosols: University of Tennessee, Department of Geological Sciences, *Studies in Geology no. 23*, 65 p.
- Olsen, P.E., 1997, Stratigraphic record of the early Mesozoic breakup of Pangea in the Laurasia-Gondwana rift system: *Annual Review of Earth and Planetary Sciences*, v. 25, p. 337-401.
- Parrish, J.T., 1993, Climate of the supercontinent Pangea: *Journal of Geology*, v. 101, p. 215-253.
- Platt, N.H., 1989, Lacustrine carbonates and pedogenesis: sedimentology and origin of palustrine deposits from the Early Cretaceous Rupelo Formation, W Cameros Basin, N Spain: *Sedimentology*, v. 36, p. 665-684.
- Platt, N.H., 1992, Fresh-water carbonates from the lower Freshwater Molasse (Oligocene, western Switzerland): *Sedimentology and stable isotopes: Sedimentary Geology*, v. 78, p. 81-99.
- Platt, N.H., and Wright, V.P., 1991, Lacustrine carbonates: facies models, facies distributions and hydrocarbon aspects; *in* Anadón, P., Cabrera, L., and Kelts, K., eds., Lacustrine facies analysis: International Association of Sedimentologists, *Special Publication 13*, p. 57-74.
- Platt, N.H., and Wright, V.P., 1992, Palustrine carbonates and the Florida Everglades: Towards an exposure index for the fresh-water environment?: *Journal of Sedimentary Petrology*, v. 62, p. 1058-1071.
- Sanz, M.E., Alonso-Zarza, A.M., and Calvo, J.P., 1995, Carbonate pond deposits related to semi-arid alluvial systems: Examples from the Tertiary Madrid Basin, Spain: *Sedimentology*, v. 42, p. 437-452.
- Spielmann, J.A. and Lucas, S.G., 2009, Triassic stratigraphy and biostratigraphy in Socorro County, New Mexico: *New Mexico Geological Society, Guidebook 60*, p. 213-226.
- Stewart, J.H., Poole, F.G., and Wilson, R.F., 1972, Stratigraphy and origin of the Chinle Formation and related Upper Triassic strata in the Colorado Plateau region: U.S. Geological Survey, *Professional Paper 690*, 336 p.
- Sucheckí, R.K., Hubert, J.F., and De Wet, C.B., 1988, Isotopic imprint of climate and hydrogeochemistry on terrestrial strata of the Triassic--Jurassic Hartford and Fundybasins: *Journal of Sedimentary Petrology*, v. 58, p. 801-811.
- Talbot, M.R., 1990, A review of the paleohydrological interpretation of carbon and oxygen isotopic ratios in primary lacustrine carbonates: *Chemical Geology*, v. 80, p. 261-279.
- Talbot, M.R., and Kelts, K., 1990, Paleolimnological signatures from carbon and oxygen isotopic ratios in carbonates from organic rich lacustrine sediments; *in* Katz, B.J., ed., Lacustrine exploration: case studies and modern analogues: American Association Petroleum Geologist *Memoir 50*, pp. 99-112.

- Tanner, L.H., 1996, Pedogenic record of Early Jurassic climate in the Fundy rift basin, eastern Canada: Museum of Northern Arizona, Bulletin 60, p. 565-574.
- Tanner, L.H., 2000, Palustrine-lacustrine and alluvial facies of the (Norian) Owl Rock Formation (Chinle Group), Four Corners Region, southwestern U.S.A.: Implications for Late Triassic paleoclimate: *Journal of Sedimentary Research*, v. 70, p. 1280-1289.
- Tanner, L.H., 2010, Terrestrial carbonates as indicators of palaeoclimate; *in* Alonso-Zarza, A.M., and Tanner, L.H., eds., Carbonates in continental settings: geochemistry, diagenesis and applications: Elsevier, Amsterdam, *Developments in Sedimentology* 62, p. 179-214.
- Tanner, L.H., and Lucas, S.G., 2006, Calcretes of the Upper Triassic Chinle Group, Four Corners region, southwestern U.S.A.: Climatic implications; *in* Alonso-Zarza, A.M., and Tanner, L.H., eds., Paleoenvironmental record and applications of calcretes and palustrine carbonates: Geological Society of America, Special Paper 416, p. 53-74.
- Tanner, L.H., and Lucas, S.G., 2007, Origin of sandstone casts in the Upper Triassic Zuni Mountains Formation, Fort Wingate, New Mexico: New Mexico Museum of Natural History and Science, Bulletin 40, p. 209-214.
- Tanner, L.H., and Lucas, S.G., 2012, Carbonate facies of the Upper Triassic Ojo Huelos Member, San Pedro Arroyo Formation (Chinle Group), southern New Mexico: Paleoclimatic implications: *Sedimentary Geology*, v. 273-274, p. 73-90.